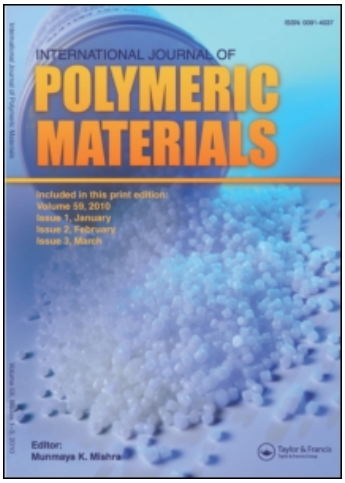

International Journal of Polymeric Materials
Publication details, including instructions for authors and subscription information:
http://www.informaworld.com/smpp/title~content=t713647664

The Effect of Nanosized Layered Materials on the Structure-Property Relationship of Poly(aniline)s: An FTIR Kinetic Study

R. Anbarasan[ab]; K. Manjula[c]; V. Vimala[c]; I. Baskaran[c]; V. Dhanalakshmi[b]
[a] Department of Mechanical Engineering, MEMS Thermal Control Lab, National Taiwan University, Taipei, Taiwan, Republic of China [b] Department of Polymer Technology, KCET, Virudhunagar, Tamil Nadu, India [c] Department of Chemistry, S.N. College, Madurai, Tamil Nadu, India

Online publication date: 03 January 2011

To cite this Article Anbarasan, R. , Manjula, K. , Vimala, V. , Baskaran, I. and Dhanalakshmi, V.(2011) 'The Effect of Nanosized Layered Materials on the Structure-Property Relationship of Poly(aniline)s: An FTIR Kinetic Study', International Journal of Polymeric Materials, 60: 2, 174 — 198
To link to this Article: DOI: 10.1080/00914037.2010.504169
URL: http://dx.doi.org/10.1080/00914037.2010.504169

International Journal of Polymeric Materials, 60:174–198, 2011

ISSN: 0091-4037 print/1563-535X online
DOI: 10.1080/00914037.2010.504169

Taylor & Francis
Taylor & Francis Group

The Effect of Nanosized Layered Materials on the Structure-Property Relationship of Poly(aniline)s: An FTIR Kinetic Study

R. Anbarasan,[1,3] K. Manjula,[2] V. Vimala,[2] I. Baskaran,[2] and V. Dhanalakshmi[3]

[1]Department of Mechanical Engineering, MEMS Thermal Control Lab, National Taiwan University, Taipei, Taiwan, Republic of China
[2]Department of Chemistry, S.N. College, Madurai, Tamil Nadu, India
[3]Department of Polymer Technology, KCET, Virudhunagar, Tamil Nadu, India

Aniline (ANI) was chemically polymerized in the presence of two different nanosized layered materials, zirconylphosphate (ZP) and molyptic acid (MA) under different experimental conditions with nitrogen purging at 45°C. The effect of nanosized layered materials on the rate of polymerization (R_p) and Fourier transform infra red-relative intensities (FTIR-RI) of benzenoid and quinonoid forms of poly(aniline) (PANI) were tested. The thermal stability and electrical conductivity values were boosted with the help of nanosized materials. High resolution transmission electron microscope (HRTEM) determined the size of nano material and its uniform distribution on the PANI matrix. For the sake of comparison, o-toluidine (OT) was polymerized under the same experimental conditions and its structure-property relationship in the presence of nano materials were also tested and critically compared with PANI systems.

Keywords FTIR, HRTEM, layered materials, poly(aniline)s, TGA

Received 23 March 2010; accepted 2 June 2010.
Address correspondence to R. Anbarasan, Department of Mechanical Engineering, MEMS Thermal Control Lab, National Taiwan University, Taipei 10617, Taiwan, ROC. E-mail: anbu_may3@yahoo.co.in

INTRODUCTION

Nowadays interest in the synthesis and characterization of conducting polymer-nano composites has increased enormously, as new hybrid materials with excellent physical, chemical, thermal and mechanical properties superior to the pristine polymer. The increase in the physical, chemical and mechanical properties of conducting polymers after making nanocomposites with layered nanosized materials urged us to do the present investigation. Naikzad and coworkers [1] synthesized PANI-exfoliated graphite nanocomposite and characterized it with FTIR, XRD, SEM and TEM. Structural and electrical properties of Ag entrapped PANI was reported by Nesher et al. [2]. Anti-corrosion properties of super paramagnetic PANI-Fe_2O_3-NiO nanocomposite were reported in the literature [3]. Cheng and the research team [4] studied the electro-rheological characteristics of PANI/titanate nanocomposites. PANI/ZnO nanocomposite was synthesized and its dielectric behavior was studied [5]. The application of PANI/Fe_3O_4 nanocomposite in microwave absorption was reported by Yang et al. [6]. The PANI/MoO_3 nanocomposite report is also available in the literature [7]. Other authors also have reported the PANI nanocomposite with WO_3 [8], TiO_2 [9], $HTiNbO_5$ [10], MWCNT [11] and Al_2O_3 [12]. Recently Anbarasan and his research team reported on the conducting polymer nanocomposites with clay [13,14] and Sb_2O_3 [15]. After by a thorough survey of the literature, we could not find any report on the PANI/ZP nanocomposite.

The added layered nanosized material altered the chemical structure of PANI. We know that the structure of PANI is made up of benzenoid and quinonoid forms, and the amount of the same can be determined by chemical and analytical methods. The chemical method consumes lot of toxic and hazardous solvents and leads to environmental pollution problems. Hence, we preferred the analytical method, particularly FTIR spectroscopy, to find out the amount of benzenoid and quinonoid forms of PANI. The FTIR spectrometer is a useful tool in various science and engineering fields, because of its high sensitivity or detectivity and low noise to signal ratio; also this method is easy and inexpensive. FTIR spectroscopy is used for both qualitative [16–19] and quantitative [20–29] analysis. By thorough literature survey, we could not find any report based on the FTIR-relative intensity (RI) based kinetics of the effect of nanosized MA and ZP on the structure-property relationship of PANI. In the present investigation, for the first time, we are reporting here on the synthesis of PANI/ZP, PANI/MA, POT/ZP and POT/MA nanocomposites in the presence of a chemical initiator and its role on the structure and property relationship of PANI and POT. Studies on the effect of nanosized ZP and MA on the structure-property relationship of PANI is the primary aim of the present investigation. In addition, the kinetics results were verified with the FTIR spectroscopic technique.

EXPERIMENTAL

Materials

Aniline (ANI) and o-toluidine (OT) monomers were purchased from Merck, India. In order to remove the inhibitor present in the monomer solution, it was distilled under vacuum prior to polymerization reaction. Hydrochloric acid (HCl, Reachem, India) and potassium peroxy disulphate (PDS, Ottokemi, India) were used without subjecting them to any further purification processes. Zirconium phosphate (ZP, SD Fine Chemicals, India) and molypdic acid (MA, Reachem) were purchased and used without further purification.

Polymer Synthesis

20 mL of ANI (1 M) in 1 M HCl was taken in a polymerization reactor and de-aerated by purging sulphur-free nitrogen gas for 30 min. The reactor was charged with 30 mL of 1 M HCl to adjust the ionic strength. The polymerization was initiated by the addition of 10 mL of a pre-aerated oxidizing agent such as PDS (0.10 M). The addition of the oxidizing agent was taken as the starting time. The reaction mixture was found to turn green in color and the appearance of the polymer formation was noticed. Polymerization was carried out at 45°C for the reaction time of two hours. After two hours of polymerization time, air was blown into the reactor to arrest the further polymerization reaction. PANI thus obtained was filtered through a previously weighed G4 sintered crucible and dried at 80°C for 6 h in the hot air oven. After drying, the crucible with polymer was weighed and the weight of the empty crucible was deducted. The difference in weight gave the weight of the formed polymer. The same method was adopted for the synthesis of PANI/ZP and PANI/MA nanocomposites by adding the different % weight of ZP or MA in the presence of PDS as an initiator. The same procedure was adopted for the synthesis of POT/ZP and POT/MA nanocomposites. The rate of polymerization (R_p) was determined by gravimetric method as follows:

$$R_P = \frac{\text{Weight of polymer obtained}}{V \times t \times M} \times 1000 \qquad (1)$$

where, V - volume of reaction mixture, t - reaction time, M - molecular weight of monomer used. The key points behind the present investigation are mentioned below:

1. The added nano material catalyzed the polymerization reaction and altered the structure of PANI.
2. The added nano material acted as a host, accommodated the PANI chains in its interlayer space, and hence confirmed the chemical interaction among them.

3. ZP or MA in its nano size accelerated the thermal and electrical conductivity values of PANI. These three things are entirely a new one from the previous literature. These are the specific reasons for the selection of ZP and MA as a nano material.

Characterization Methods

FTIR spectra of PANI and POT samples in disc form were recorded by using a Shimadzu 8400 S FTIR spectrophotometer instrument. 3 mg of PANI powder sample was well grinded with 250 mg of KBr and made into a disc by pressing. After recording the spectrum, the baseline correction was made carefully and the corrected area of the peaks was determined using FTIR software. For the quantitative determination of % amino and imino forms of PANI, the following areas of the peaks, which were assigned at 1490 (benzenoid form), 1590 (quinonoid form) and 809 (C-H out of plane bending vibration) cm^{-1} were determined and the RI was calculated as follows:

$$\text{Relative intensity of benzenoid form} = A_{1490}/A_{809} \quad (2)$$

$$\text{Relative intensity of quinonoid form} = A_{1590}/A_{809} \quad (3)$$

In order to avoid error while recording the FTIR spectrum, the corrected peak area was considered and the value for the above-mentioned peak was noted. To crosscheck the corrected peak area values, the FTIR spectra were recorded for the same sample disc in different parts. After proper base line correction with the aid of FTIR software, again one can get the same corrected peak area values. The FTIR spectrum was recorded three times for the same sample disc, and one gets same and repeated corrected peak area values. The FTIR spectrum was recorded without predicting the lower and upper limits of peaks, because the software itself predicted exactly the lower and upper limits to nullify the errors. In such a way the errors were nullified. Further one can crosscheck the efficiency of FTIR software by manually predicting the lower and upper limits and the corrected peak area was determined. In this case, one can get the same corrected peak area value as reported previously (without predicting the lower and upper peak limits). TGA analysis was performed under air purge at the heating rate of 10°C/min by using SDT 2960 simultaneous TGA and DSC, TA Instruments. Standard four probe method was used for the determination of conductivity value of polymer samples. HRTEM was recorded by using a (TEM 3010) transmission electron microscopy (TEM) instrument, a product of JEOL.

RESULTS AND DISCUSSION

Effect of Time on the R_p and RI of Benzenoid and Quinonoid Forms of PANI

ANI was polymerized at different time intervals from 3000 to 18000 sec, whereas the other experimental conditions were kept constant. While increasing the reaction time interval, the R_p value was increased for both ANI-PDS-ZP and ANI-PDS-MA systems. This can be attributed to the following factors:

1. longer reaction time interval activated the coupling of aniline radical cations,
2. favored the interaction between ANI, PDS and nano materials, and
3. provided the possible conversion of benzenoid into more rigid quinonoid structure.

Figure 1(a) shows the plot of time vs. R_p for ANI-PDS-ZP system. The plot showed a straight line but with a decreasing trend. This is due to the presence of bulk value in the denominator of rate determining equation.

ANI was polymerized in the presence of another nanosized material, namely MA. Here also the above-mentioned experimental conditions were maintained. While increasing the reaction time, the R_p value was also increased due to the various possible coupling reactions. Figure 1(b) shows

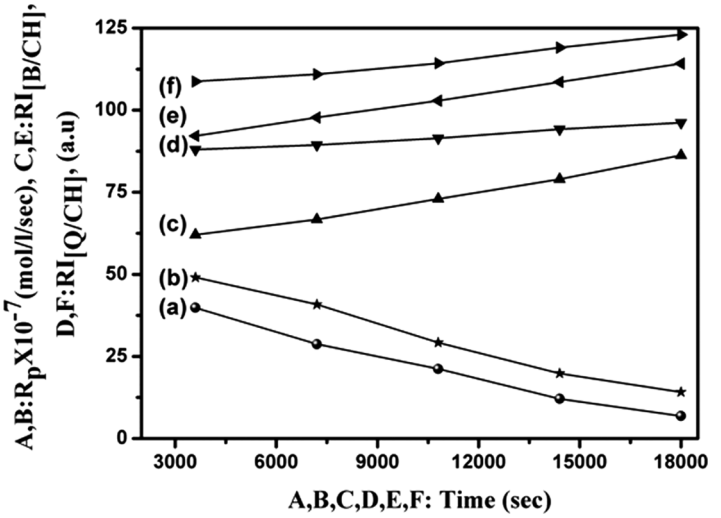

Figure 1: Effect of time on (a,b) R_p, (c,d) $RI_{(B/CH)}$, and (e,f) $RI_{(Q/CH)}$ (ANI) = 0.025 M, (PDS) = 0.025 M, and Temperature = 45°C, (a,c,e-ANI-PDS-ZP), (b,d,f-ANI-PDS-MA).

the plot of time vs. R_p for MA system. The above said observation was noted here. In comparison, the ZP system exhibited the higher R_p value due to surface catalytic effect.

PANI synthesized under the above-mentioned experimental condition was subjected to FTIR spectroscopy. Spectral details are given in the FTIR characterization part. The effect of reaction time on the PANI backbone formation was analyzed with the help of FTIR spectroscopy. Figure 1(c) shows the plot of time vs. $RI_{[B/CH]}$ for the ANI-PDS-ZP system. The plot showed a straight line which indicated that the RI was increased simultaneously with the reaction time. The increase in RI confirmed the polymerization of ANI and resulted in higher molecular weight PANI. (The GPC measurement is going on in our lab to confirm the molecular weight of PANI). The increase in the RI of [B/CH] was caused by the various possible coupling reactions. Figure 1(d) explains the plot of time vs. $RI_{[Q/CH]}$, here also one can observe the above-mentioned trend. The RI of [Q/CH] was increased with the time by the secondary oxidation or over oxidation reactions. The present system exhibited higher RI values for the benzenoid structure formation reaction rather than the quinonoid structure formation reaction due to the lower oxidation potential of the primary oxidation reaction. This is in accordance with our recent publication [27].

ANI was polymerized in the presence of MA also. The above plots were made for this system too. Time vs. $RI_{[B/CH]}$ (Figure 1(e)) and time vs. $RI_{[Q/CH]}$ (Figure 1(f)) plots were made. The plots showed straight lines with a linear increasing trend. This authenticated that ANI was polymerized in the presence of both PDS and MA. The increase in RI is due to the following reasons: primary oxidation, secondary oxidation, over oxidation, thermal oxidation reactions, auto acceleration effect caused by the PANI and surface catalytic effect provided by the nanosized host material, complex forming behavior of nano material, and intercalation of PANI chains into the basal spacing of nano material. The ANI-PDS-MA system pointed out that the RI value of the benzenoid form is greater than that of the quinonoid form. In overall comparison, the former system provided higher RI values for the benzenoid form. This is due to the higher surface catalytic effect of ZP than MA and better dissolution of ZP in the given reaction medium. The effect of time on the RI of benzenoid and quinonoid forms of PANI are similar to the report of Radhika et al. [27].

Effect of (ANI) on the R_p and Benzenoid and Quinonoid Forms of PANI

ANI was polymerized under different [ANI]. While keeping other experimental conditions constant, the [ANI] was varied between 0.69 and 1.17 M.

While increasing the [ANI], the R_p value was increased for both MA and ZP systems. This can be explained based on the following reasons:

1. availability of more monomeric units,
2. auto acceleration effect caused by the formed PANI surface,
3. catalytic effect caused by the surface of nanosized material, and
4. generation of more and more anilinium radical cations in the reaction medium.

In comparison, the ANI-PDS-ZP system exhibited higher R_p value than the ANI-PDS-MA system. This can be explained on the basis of

1. better dissolution of ZP in the given reaction medium,
2. complex formation of ZP with ANI and PDS molecules,
3. accommodation of more number of ANI units in its interlayer space, and it exhibited a good host nature.

In the case of MA, viscosity of the reaction medium increased and hence resulted in restriction in the coupling of anilinium radical cations. Also, it can accommodate a lesser number of monomeric units in its basal spacing. In order to find out the order of reaction, the plot of log [ANI] vs. logR_p (Figure 2(a)) was made for the ZP system. The plot indicated a straight line with the slope value 0.76, which confirmed the 0.75 order of reaction with respect to [ANI]. The same type of plot was made for the MA system as in

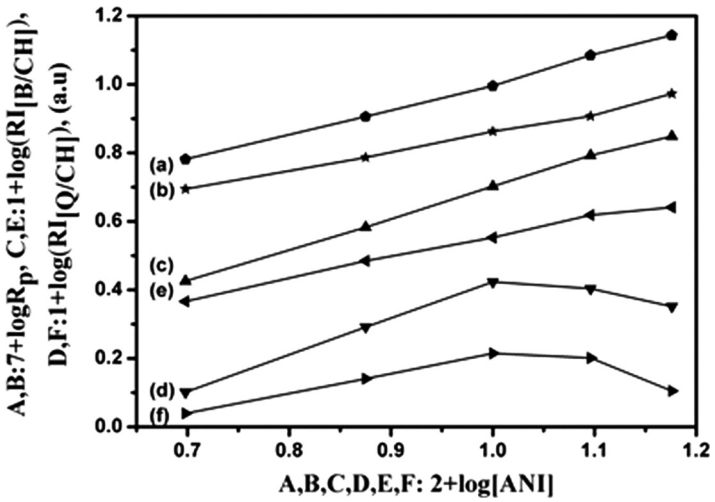

Figure 2: Effect of (ANI) on (a,b) R_p, (c,d) $RI_{(B/CH)}$, and (e,f) $RI_{(Q/CH)}$ (PDS) = 0.025 M, Temperature = 45°C, Time-2 h (a,c,e-ANI-PDS-ZP), (b,d,f-ANI-PDS-MA).

Figure 2(b) {log[ANI] vs. logR_p}. Here also the plot indicated a straight line with the slope value of 0.57 that confirmed the 0.50 order of reaction with respect to [ANI]. The reason for the best performance of ZP was explained above. The results are in accordance with the literature [13,27].

The above synthesized samples were subjected to FTIR analysis. While increasing the concentration of ANI, the RI of benzenoid structure was increased. The increase in RI of the benzenoid form confirmed the polymerization reaction of ANI. In order to find out the order of benzenoid structure formation reaction, for ZP system, the log-log plot was made, i.e., the plot of log[ANI] vs. log($RI_{[B/CH]}$) (Figure 2(c)) was done and the slope value was determined from the straight line as 0.90. This indicated the first order reaction of benzenoid structure formation with respect to [ANI]. After $M/I = 1$, the excess ANI was subjected to primary oxidation by the auto acceleration and surface catalytic effects. Hence, the RI of benzenoid form was continuously increased with the increase of [ANI]. In addition, we know that benzenoid and quinonoid forms combined to build up PANI backbone. Let us analyze the effect of [ANI] on the quinonoid structure formation. While increasing the concentration of ANI, the RI of the quinonoid structure formation was also increased up to ANI concentration of 1.0 M. Thereafter, the RI value of quinonoid form was decreased. This is due to the following reasons:

1. quinonoid forms were obtained because of secondary or over oxidation reactions,
2. when $[M/I] = 1$ is attained, no more free radicals are available for the secondary oxidation reaction,
3. due to the requirement of higher activation energy for the quinonoid structure formation, and
4. the auto catalytic effect (due to the formed PANI surface) and surface catalytic effect (due to the nanosized material) are not effectively acted for the quinonoid structure formation. Plotting log[ANI] vs. log($RI_{[Q/CH]}$) (Figure 2(d)) helped us to find the order of quinonoid structure formation as 0.57.

This explained that the quinonoid structure formation followed the 0.50 order of reaction with respect to [ANI]. In this system, the slope value was determined from the increasing linear region of Figure 2(d). In comparison, the RI values of the benzenoid structure are greater than that of the quinonoid form of PANI. This is attributed to the surface catalytic effect [27] of ZP and the auto acceleration effect of formed PANI.

ANI was polymerized under different concentrations in the presence of MA. In this system also the above said trend was observed. The order of benzenoid and quinonoid structure formation was determined from the slopes

of the following plots. Log [ANI] vs. log($RI_{[B/CH]}$) (Figure 2(e)) and log [ANI] vs. log($RI_{[Q/CH]}$) (Figure 2(f)), the slope values were calculated as 0.58 and 0.51, respectively, for benzenoid and quinonoid structure formation for the MA system. These slope values declared that both benzenoid and quinonoid forms of PANI backbone formation followed the 0.50 order of reaction with respect to [ANI]. In the case of the MA system, the RI value of the benzenoid structure is greater than that of the quinonoid structure of PANI. Again, this explained the lower oxidation potential required for the primary oxidation reaction [27]. In overall comparison, the ZP system showed higher RI values than the MA system. This is due to the better complex formation as well as catalytic behavior of ZP than MA.

Effect of (PDS) on the R_p and Benzenoid and Quinonoid Forms of PANI

PANI was synthesized under various concentrations of initiator, PDS, while the other experimental conditions were constant. While increasing the concentration of PDS from 0.69 to 1.17 M, the R_p value was increased. The following points supported the increasing trend:

1. the availability of more and more initiator radicals for the polymerization reaction, and
2. coupled effects of auto acceleration and catalytic effects.

The ZP system showed slightly higher R_p values than MA system. This explained the better complex formation between ZP, PDS and ANI molecules. The order of reaction can be determined by plotting log [PDS] vs. logR_p (Figure 3a) for the ZP system as 0.94. This explored the first order dependence of R_p with respect to [PDS]. The same type of plot was made for MA system. Log [PDS] vs. logR_p (Figure 3(b)) exhibited a straight line with a slope value of 1.22. This nominated the 1.25 order of polymerization reaction. Figures 3(a) and 3(b) indicates that 1 mole of PDS and 1.25 mole of PDS are required to oxidize one mole of ANI for ZP and MA systems, respectively. Anbarasan et al. [13], studied the effect of nanosized material on the chemical polymerization of ANI. The present investigation is in accordance with Anbarasan et al. [13].

The RI measurements were followed for the above synthesized samples. The RI value for the benzenoid structure of the ZP system was initially increased and thereafter it showed a decrement value. This can be accounted by the fact that at higher [PDS], there were still more free radicals available for the secondary reactions. Once all the monomers were primarily oxidized, the ANI moieties were further subjected to the secondary oxidation reaction and resulted in a decrease in concentration of benzenoid structure.

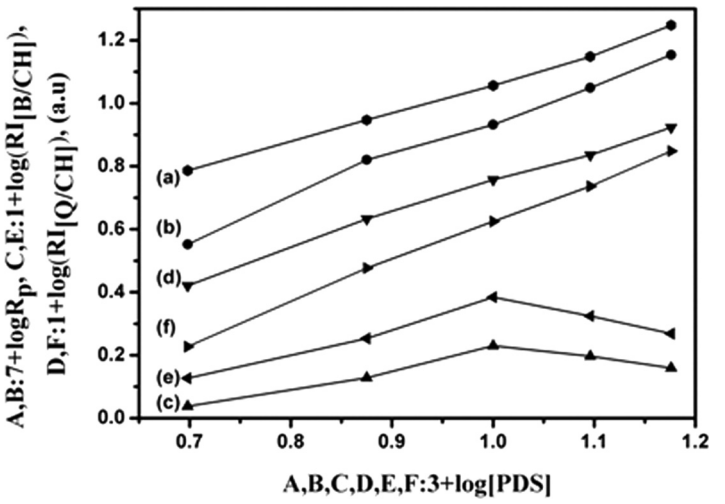

Figure 3: Effect of (PDS) on (a,b) R_p, (c,d) $RI_{(B/CH)}$, and (e,f) $RI_{(Q/CH)}$ (ANI) = 0.025 M, Time-2 h, Temperature = 45°C, (a,c,e-ANI-PDS-ZP), (b,d,f-ANI-PDS-MA).

Figure 3(c) proves the above said fact for the ZP system. As usual, the order of benzenoid structure formation reaction can be determined by plotting log [PDS] vs. log ($RI_{[B/CH]}$) (Figure 3(c)). The plot showed two regions and the slope value was determined from the linear increasing region as 0.62. This confirmed the 0.50 order of benzenoid structure formation reaction with respect to [PDS]. It means that 0.50 mole of initiator is required to oxidize 1 mole of ANI monomer. Similarly the order of quinonoid structure formation reaction was determined by plotting log [PDS] vs. log ($RI_{[Q/CH]}$) (Figure 3(d)). The plot showed a straight line with a slope value of 0.84, which recommended the first order quinonoid structure formation reaction with respect to [PDS], i.e., 1 mole of PDS is required to form 1 mole of quinonoid structure of PANI. The continuous increase in RI of [Q/CH] is due to the secondary or over oxidation reactions [27]. In comparison, the RI value of the quinonoid structure is greater than that of the benzenoid structure due to the availability of more and more active sites for the further oxidation reactions.

Same plots were applicable for the MA system too. The above said trend is observed here also for both benzenoid and quinonoid structure formation of PANI. Log [PDS] vs. log ($RI_{[B/CH]}$) (Figure 3e) and log [PDS] vs. log ($RI_{[Q/CH]}$) (Figure 3(f)). The slope values were estimated as 1.03 and 1.27 for benzenoid and quinonoid forms of PANI, respectively. This informed us that the benzenoid structure formation followed the first order reaction, whereas the quinonoid structure formation followed the 1.25 order of reaction with respect to [PDS]. Moreover, 1.27 mole of PDS is required to form 1 mole of quinonoid structure of PANI. In comparison, the PANI-ZP system yielded better results than the

PANI-MA system. Again, this confirmed the surface catalytic effect and host nature of ZP.

Effect of Temperature on the R_p and Benzenoid and Quinonoid Forms of PANI

ANI was polymerized at different temperatures while the other experimental conditions were kept constant. When the temperature was increased, the R_p was also increased, for both systems. The increase in R_p is mainly due to the thermal oxidation reaction. As usual, the R_p value for the ZP system showed higher R_p value than the MA system due to the effective catalytic activity of ZP. In order to find out the energy of activation (E_a), 1/T vs. logR_p (Figure 4(a)) was made for the ZP system. The E_a value was calculated from the slope value as 280.2 kJ/mol, whereas the MA system noticed the E_a value of 325.3 kJ/mol (1/T vs. logR_p) (Figure 4(b)). The ZP system consumed lower amounts of thermal energy for the thermal oxidation of ANI monomer than the MA system. Consumption of lower amounts of heat energy favored the R_p.

The E_a value for the benzenoid and quinonoid structure formation was determined for ZP and MA systems. Figure 4(c) represents the plot of 1/T vs. log($RI_{[B/CH]}$) for ZP system. While increasing the temperature, the RI of [B/CH] was also increased up to a maximum level and then it showed a decreasing trend. The benzenoid structure formation was followed by the primary oxidation reaction, whereas at a higher temperature the secondary

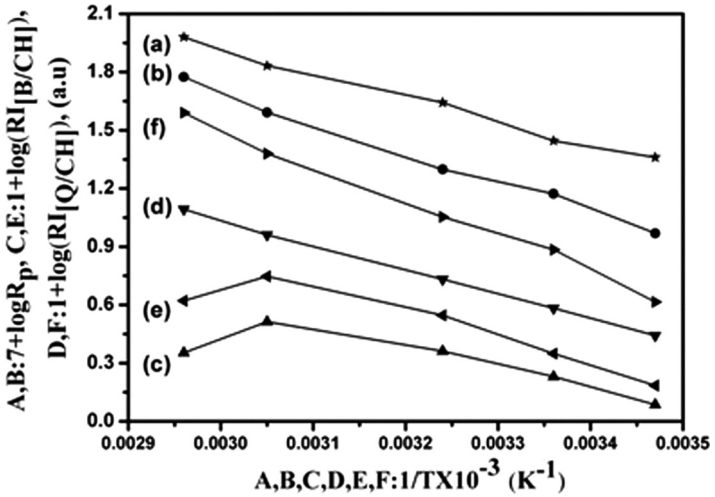

Figure 4: Effect of temperature on (a,b) R_p, (c,d) $RI_{(B/CH)}$, and (e,f) $RI_{(Q/CH)}$ (ANI) = 0.025 M, Time-2 h, (PDS) = 0.025 M, (a,c,e-ANI-PDS-ZP), (b,d,f-ANI-PDS-MA).

oxidation, over oxidation or thermal oxidation played a vital role and resulted in the conversion of benzenoid structure into quinonoid structure [27]. Hence, at higher temperatures the concentration of the benzenoid form was found to be decreased. The E_a value was calculated from the slope for the above-mentioned plot as 231.68 kJ/mol. The E_a value for the quinonoid structure formation of PANI can be determined from the plot of 1/T vs. $\log(RI_{[Q/CH]})$ (Figure 4(d)) as 271.44 kJ/mol. These E_a values concluded that benzenoid structure formation consumed lower amounts of thermal energy, whereas the quinonoid structure formation consumed higher amounts of thermal energy. Similarly, the E_a values for the MA system were determined from the plots of 1/T vs. log $(RI_{[B/CH]})$ (Figure 4(e)) and 1/T vs. $\log(RI_{[Q/CH]})$ (Figure 4(f)) as 290.4 and 320.7 kJ/mol respectively. This system also consumed a lower amounts of thermal energy, for benzenoid structure formation. This is in accordance with the reported literature [27].

In comparison, the ZP system consumed a lower amount of thermal energy for the formation of both benzenoid and quinonoid structure formation due to low de-stacking energy as well as the surface catalytic effect of ZP. Moreover, the E_a values obtained from the R_p as well as RI methods are nearly equal to each other. This inferred that one can find out the E_a value from the FTIR-RI method also instead of R_p, or otherwise one can crosscheck the E_a values calculated from those two methods.

Effect of (% Weight of ZP or MA) on the R_p and Benzenoid and Quinonoid Forms of PANI

The % weight of ZP was increased from 1 to 5% weight while the other experimental conditions were kept constant. While increasing the % weight of ZP, the R_p value was increased. This trend is in accordance with the literature [27]. The increase in R_p can be expressed interms of the following factors:

1. due to the nano size of ZP, the surface catalytic effect played a vital role,
2. excellent interaction between ANI, PDS and ZP molecules,
3. exfoliation or delamination easily occurred in the given experimental conditions,
4. low de-stacking energy of ZP,
5. accommodation of a greater number of monomer molecules, and
6. better dissolution in the given experimental conditions.

In order to find out the order of reaction, the following log-log plot was made, i.e., plot log(% weight of ZP) vs. $\log R_p$ (Figure 5(a)). The plot exhibited a straight line with the slope value of 0.88, which tutored the first order

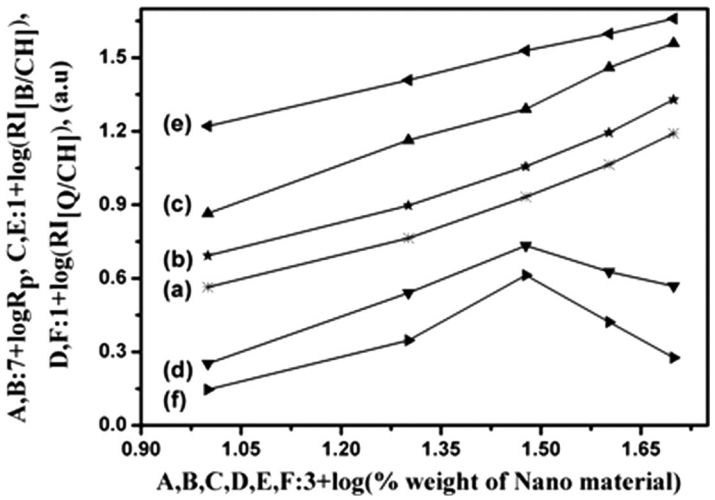

Figure 5: Effect of (% weight of nano material) on (a,b) R_p, (c,d) $RI_{(B/CH)}$, and (e,f) $RI_{(Q/CH)}$ (ANI) = 0.025 M, (PDS) = 0.025 M, Time-2 h, Temperature = 45°C, (a,c,e-ANI-PDS-ZP), (b,d,f-ANI-PDS-MA).

reaction with respect to % weight of ZP. The MA system too indicated the first order reaction from the plot of log(% weight of MA) vs. logR_p (Figure 5(b)). In comparison, the ZP system showed higher surface catalytic activity than the MA system due to the above-mentioned reasons.

The effect of % weight of ZP on the FTIR behavior of PANI was tested. It was noted that the RI of the benzenoid formation increased with the increase of % weight of ZP. This explained the surface catalytic effect with mild oxidizing behavior of ZP. The order of benzenoid structure formation can be determined by making a plot of log(% weight of ZP) vs. log($RI_{[B/CH]}$) (Figure 5(c)). The plot indicated a straight line with a slope of 0.98, again which confirmed the first order reaction with respect to % weight of ZP. This gives an idea that 1 mole of ZP is required to form 1 mole of benzenoid structure. While increasing the % weight of ZP, the RI of quinonoid structure was increased initially and reached a maximum value at 3 weight % and thereafter it showed a decreasing trend. Radhika et al. explain the details for this trend [27]. The decrease in RI of the quinonoid form is explained here. The highly active nature of the ZP surface led to the primary oxidation reaction and resulted in a higher quantity of benzenoid form. In the presence of ZP and PDS molecules, it also favored the primary oxidation reaction rather than the secondary or over oxidation reactions. This is due to the higher oxidation potential of the secondary oxidation reaction. This resulted in the formation of more and more benzenoid structure formations. In order to find out the order of quinonoid structure formation, the plot of log(% weight of ZP) vs. log($RI_{[Q/CH]}$) (Figure 5(d)) was made and the slope value was determined as 0.62. This

convinced the 0.50 order of quinonoid structure formation with respect to % weight of ZP. 0.50 mole of ZP is required to form 1 mole of quinonoid structure. In comparison, the ZP system posed higher RI values than the MA system due to the above said reasons.

The effect of % weight of MA on the FTIR spectroscopy was analyzed. Figures 5(e) and 5(f) shows the plots of log(% weight of MA) vs. log($RI_{[B/CH]}$) and log(% weight of MA) vs. log($RI_{[Q/CH]}$) respectively, with the slope value of 1.0 of 0.94. This pin pointed the first order dependence of both benzenoid and quinonoid forms of PANI with respect to % weight of MA. In comparison, the ZP system showed higher RI values than the MA system due to higher surface catalytic activity and low de-stacking energy.

For the sake of comparison, OT was polymerized in the presence of different % weight of ZP and MA. The results are discussed below.

Effect of (% Weight of ZP or MA) on the R_p and Benzenoid and Quinonoid Forms of POT

OT was polymerized under different % weight of ZP, while the other experimental conditions were kept constant. The % weight of ZP was varied between 1 and 5%. It was noted that while increasing the % weight of ZP, the R_p was also increased. Again, this is due to the surface catalytic effect of ZP. Our next duty is to find out the order of ZP catalyzed OT polymerization. For this purpose, the plot of log(% weight of ZP) vs. logR_p (Figure 6(a)) was drawn and the slope value was derived as 1.0. This led to the conclusion of first

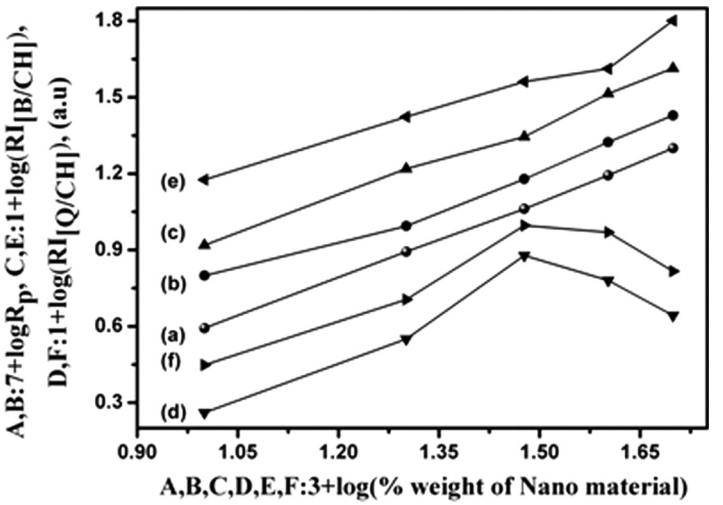

Figure 6: Effect of (% weight of nano material) on (a,b) R_p, (c,d) $RI_{(B/CH)}$, and (e,f) $RI_{(Q/CH)}$ (PDS) = 0.025 M, Temperature = 45°C, Time-2 h (a,c,e-OT-PDS-ZP), (b,d,f-OT-PDS-MA).

order dependence of R_p on % weight of ZP. Under the same experimental conditions, OT was polymerized in the presence of MA. The above said plot was made for this system too, log(% weight of MA) vs. logR_p (Figure 6(b)) and the slope value was calculated as 0.90, which confirmed the first order dependence of R_p with respect to % weight of MA. One mole of MA is required to oxidize one mole of OT. In comparison, the OT-PDS-ZP and OT-PDS-MA system produced higher R_p value than the ANI-PDS-ZP and ANI-PDS-MA systems. This is because of lower oxidation potential of OT than ANI. The lower oxidation potential of OT can be ascribed to the presence of electron releasing bulky methyl substituent present in the ortho position of OT. Moreover, the methyl group restricted the ring flipping process, ortho coupling reactions and crosslinking reactions, and hence resulted in higher R_p values than the ANI system.

The effect of methyl substituent in the ortho position of OT on the FTIR – RI was analyzed. While increasing the % weight of ZP, the RI of [B/CH] values was increased steeply. This is due to the surface catalytic effect of ZP [27]. The order of benzenoid structure formation reaction can be determined by plotting log(%weight of ZP) vs. log($RI_{[B/CH]}$) (Figure 6(c)) as 0.98. The important point noted here is the RI values are higher for OT than the ANI system. It means that the POT chain length is higher than PANI system, and automatically the M_w might be increased. The GPC measurement is under investigation in our lab. In the case of RI measurement of [Q/CH], the RI was increased with the increase of % weight of ZP up to 3 weight %, thereafter it showed a decreasing trend. This is due to the higher activation energy of secondary or over oxidation reactions. The trend is shown in Figure 6(d), log(% weight of ZP) vs. log($RI_{[Q/CH]}$). In order to find out the order of reaction, we need the slope value, the same can be obtained from Figure 6(d) in the increasing linear region as 0.83, which confirmed the unity order of reaction with respect to % weight of ZP. The same plots were made for OT-PDS-MA system, i.e., log(% weight of MA) vs. log($RI_{[B/CH]}$ (Figure 6(e)) and log(% weight of MA) vs. log ($RI_{[Q/CH]}$) (Figure 6(f)). The slope values were determined as 1.25 and 1.11. In comparison, OT-PDS-MA system showed higher order of reaction than the OT-PDS-ZP system due to very high de-stacking energy. At the same time, the RI values are higher than that of the ANI system. On overall comparison, the R_p and RI values are higher for the OT system than the ANI system due to the lower oxidation potential of OT.

FTIR Spectroscopy

Figure 7 shows the FTIR spectra of the ANI-PDS-MA system loaded with different % weight of MA. The important peaks are characterized below. A peak at 1558 cm^{-1} is due to the quinonoid structure of PANI. The benzenoid stretching appeared at 1481 cm^{-1}. The C-N stretching is shown in 1304 cm^{-1}.

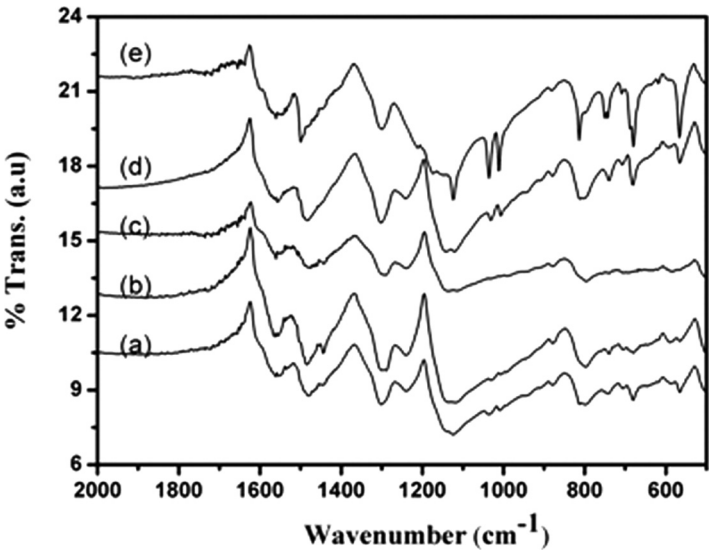

Figure 7: FTIR spectrum of PANI loaded with ZP at (a) 1% weight, (b) 2% weight, (c) 3% weight, (d) 4% weight, (e) 5% weight.

The HCl dopant can be seen at 1132 cm^{-1}. The C-H out-of-plane bending vibration appeared at 809 cm^{-1}. The Cl^- stretching appeared at 568 cm^{-1}. The metal oxide stretching is observed at 680 cm^{-1}. At 5% weight loading of MA, the characteristic peaks are well separated. In the present investigation, we give special attention to benzenoid (1481 cm^{-1}), quinonoid (1558 cm^{-1}) and C-H out-of-plane bending (809 cm^{-1}) vibration only.

Figure 8 indicates the FTIR spectra of the OT-PDS-ZP system loaded with different % weight of ZP. Here also the above said peaks appeared with some new peaks particularly, peaks appeared in the fingerprint region. A small hump at 678 cm^{-1} accounted for the PO_4^{2-} stretching.

TGA Profile

Figure 9 exhibits the TGA of the ANI-PDS-ZP system. The thermogram showed a two-step degradation process. The first minor weight loss step below 150°C is due to the removal of moisture and physisorbed water molecules. The second major weight loss step is accounting for the degradation of the PANI backbone. Figure 9(a) shows the TGA thermogram of the pristine PANI Figures 9(b-f) show the TGA of 1–5% weight of ZP-loaded PANI. The important point noted here is while increasing the % weight loading of ZP, the T_{id} as well as the % weight of residue remaining at 500°C was also increased Thus, the added nanosized ZP increased the char-forming behavior of PANI. The 1% weight ZP-loaded PANI showed 12.8% weight residue remained at 500°C, whereas the 5% weight ZP-loaded PANI exhibited 26.3% residue

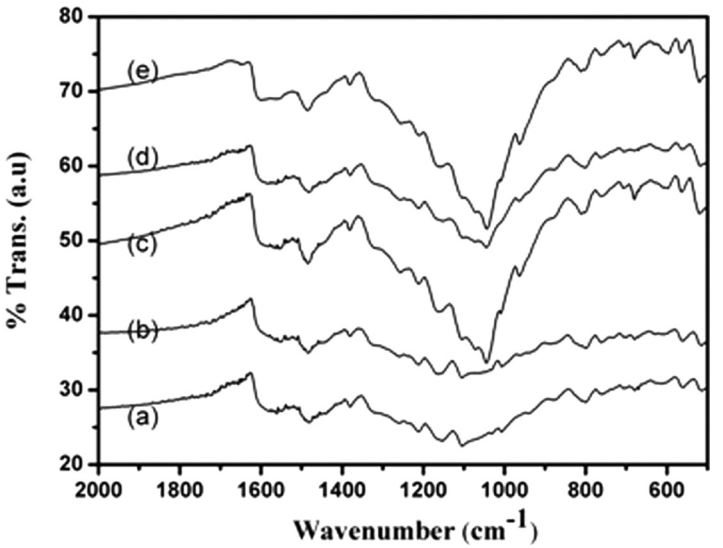

Figure 8: FTIR spectrum of POT loaded with MA at (a) 1% weight, (b) 2% weight, (c) 3% weight, (d) 4% weight, (e) 5% weight.

remained at 500°C. The increase in thermal stability confirmed the nanocomposite formation between ZP and PANI chains. In our earlier communication, the added nano material increased the char-forming tendency of poly(α-naphthylamine) [27]. The present system is also in accordance with that.

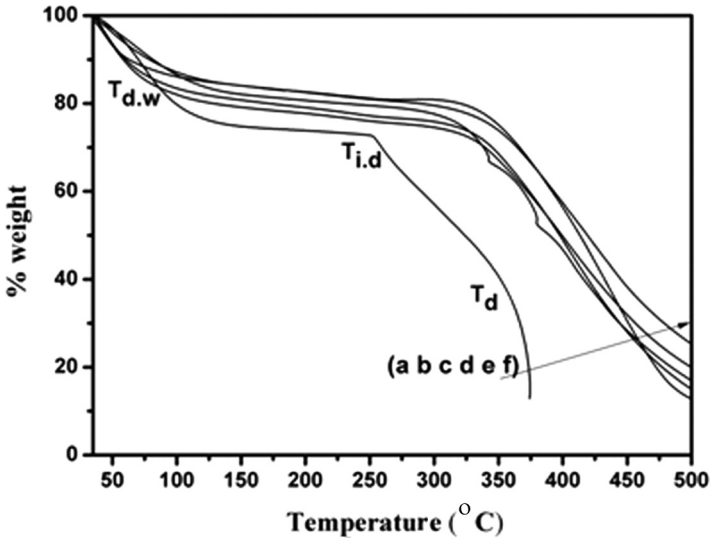

Figure 9: TGA of PANI loaded with ZP at (a) 1% weight, (b) 2% weight, (c) 3% weight, (d) 4% weight, (e) 5% weight.

Figure 10 represents the TGA thermogram of 1 to 5% weight MA loaded PANI. Figure 10(a) confirms the TGA of pristine PANI. Here also one can observe a two-step degradation process similar to PANI-PDS-ZP system. While increasing the % weight loading of MA the % weight residue remained at 400°C was also increased. The 1% weight MA-loaded PANI showed 38.5% weight residue remained whereas the 5% weight MA-loaded PANI showed 56% weight residue. This confirmed the increased in char-forming behavior of PANI when loaded with increment % weight of MA. In comparison, the MA-loaded PANI admitted higher thermal stability than the PANI-PDS-ZP system. This explained the higher thermal stability of metal oxide compared to metal phosphate. The PANI-clay nanocomposite system also exhibited the same type of results [13].

Figure 11(a) accounts for the TGA of pristine POT synthesized under the given experimental conditions. The OT-PDS-ZP system also exhibited a two-step degradation process similar to the ANI-PDS-ZP system. The first minor weight loss step up to 100°C is corresponding to the removal of moisture and physisorbed water molecules. The second major weight loss is associated with the degradation of the POT backbone. At 450°C the pristine POT showed 9.6% weight residue remained. The 1% weight ZP loaded POT showed 24% residue remained whereas the 5% weight ZP-loaded POT exhibited 57.5% (Figures 11(b–f)). This strongly supported the increase in thermal stability of POT–ZP nanocomposites. The important point noted here is the % weight residue remained at 450°C is simultaneously increased with % increment loading of ZP and the T_{id} is also increased. This explained the thermally stable nanocomposite formation between ZP and

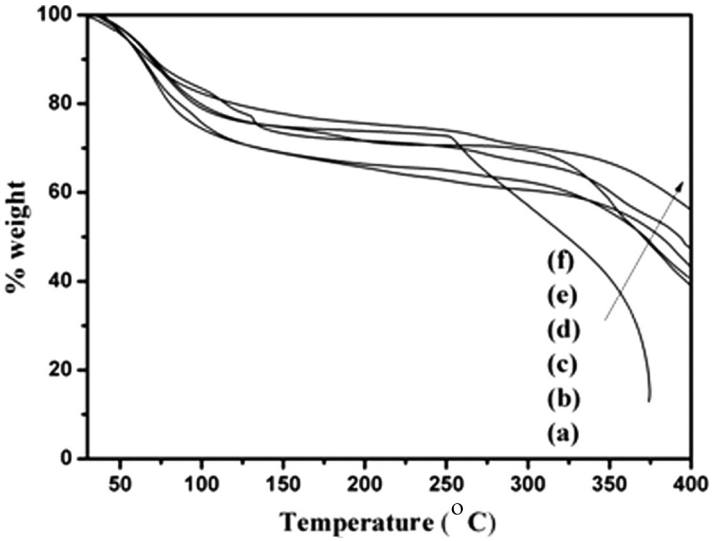

Figure 10: TGA of PANI loaded with MA at (a) 1% weight, (b) 2% weight, (c) 3% weight, (d) 4% weight, (e) 5% weight.

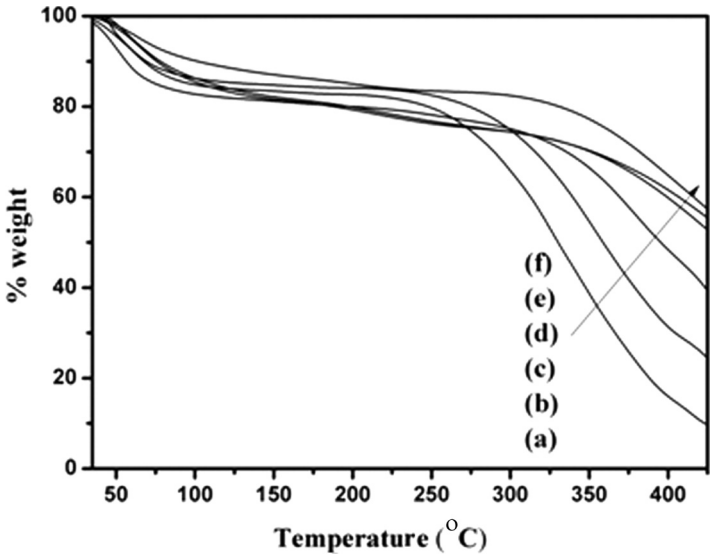

Figure 11: TGA of POT loaded with ZP at (a) 1% weight, (b) 2% weight, (c) 3% weight, (d) 4% weight, (e) 5% weight.

POT. The increase in T_{id} with the increase of % weight of clay was already reported in the literature [13]. Here also the same trend was noted.

Figure 12 exhibits the TGA of the POT-PDS-MA system. Here also the above-mentioned observations were noted. The % weight residue remained

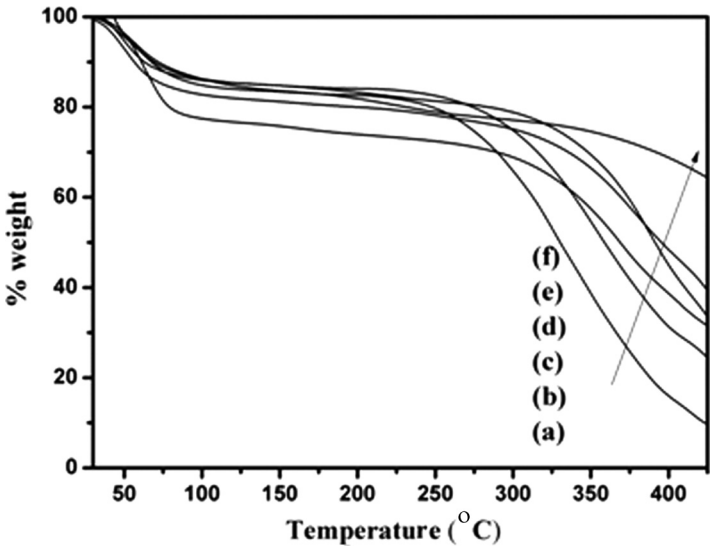

Figure 12: TGA of POT loaded with MA at (a) 1% weight, (b) 2% weight, (c) 3% weight, (d) 4% weight, (e) 5% weight.

at 425°C is 25.1 and 64.9% respectively for 1 and 5% weight MA-loaded POT (Figures 12(b–f)). In the case of POT, the MA-loaded system yielded higher thermal stability than the POT-ZP system. For the sake of comparison, the TGA of pristine POT is given in Figure 12(a).

On overall comparison, the POT system exhibited higher thermal stability than the PANI system. While comparing the thermal stability of metal oxide and metal phosphate loaded conducting polymer, the former case stood as a first member. Finally, the POT-MA system showed the best thermal stability.

Conductivity Report

The effect of % weight loading of nanosized material on the electrical conductivity of PANI and POT were checked. Pristine PANI and POT showed the electrical conductivity value of 5.32×10^{-3} S/cm and 1.29×10^{-5} S/cm, respectively. PANI and POT loaded with nanomaterials yielded good increases in electrical conductivity values. This is represented in Figure 13. While increasing the % weight loading of ZP, the electrical conductivity value of PANI was also increased. At 5% weight loading, it showed the maximum conductivity value of 10.7×10^{-2} S/cm (Figure 13(a). Figure. 13(b) indicates the plot of % weight of MA vs. conductivity value. At 5% weight loading of MA, PANI showed the electrically conductivity value of 12.4×10^{-2} S/cm. On comparison, the metal oxide (MA)-loaded PANI was embedded with higher

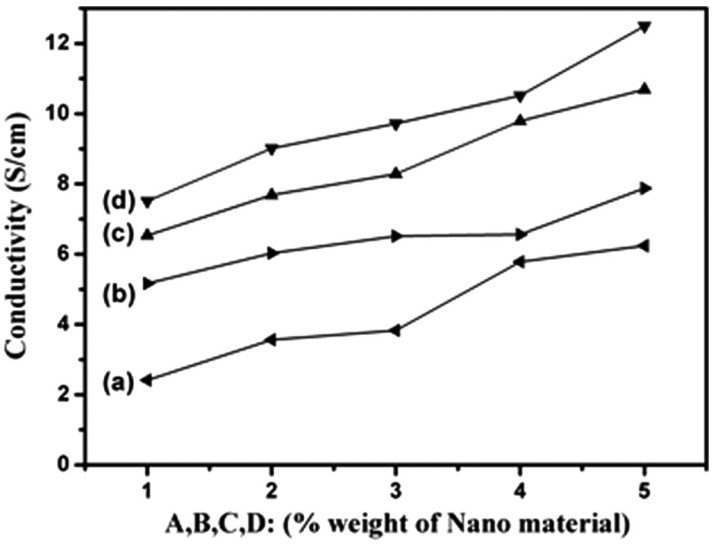

Figure 13: Conductivity value of (a) ANI-PDS-ZP, (b) ANI-PDS-MA, (c) OT-PDS-ZP, (d) OT-PDS-MA systems.

electrical conductivity values. This explained the better doping nature of MA. Recently Radhika et al. reported on the electrical conductivity value of metal oxide- loaded poly(α-naphthylamine) nanocomposites [27].

Figures 13(c) and (d) indicate the electrical conductivity value of ZP and MA loaded POT. The most interesting observation is that while increasing the % weight of nano material, the electrical conductivity value is also increased. The doping nature of nanosized material promised the increase in electrical conductivity value. As a result, the conductivity value is increased by one order of magnitude (from 2.3×10^{-4} to 6.2×10^{-4} S/cm) (Figure 13(c) for OT-PDS-ZP). The added nano material created charges on the backbone of POT via doping effect. The OT-PDS-MA system showed the maximum electrical conductivity of 7.8×10^{-4} S/cm.

On critical comparison, PANI produced higher conductivity value than its methyl substituted derivative, because the bulky methyl group led to the steric effect as well as the ring flipping effect, and hence resonance stabilization was restricted. While comparing the doping nature of MA and ZP, the former showed better results. Finally, one can say that the ANI-PDS-MA system showed higher electrical conductivity than the other systems. ZP may be a better host or catalyst, but it is a poor dopant.

HRTEM Study

The nano size and the layered structure of ZP and MA can be confirmed by HRTEM techniques. Figure 14(a) confirms the ZP size of 5–10 nm for the PANI-PDS-ZP system. The layered (partly exfoliated) structure of ZP is represented in Figure 14(b). Figure 14(c) and (d) exhibit the uniform distribution as well as layered structure with 5–15 nm length of MA nanosized particles, respectively. The breadth of single MA layer is less than 1 nm (Figure 14d). For the sake of convenience, the HRTEM of OT-PDS-ZP and OT-PDS-MA are not attached here.

Mechanism

Poly(aniline) formation proceeded through oxidative free radical initiation mechanism. We know that free radical method includes three steps, namely, initiation, propagation and termination. Our earlier publications also confirmed the same [30–32]. In the present investigation, for the first time, we are proposing a mechanism for the polymer/nanocomposites based on the FTIR-RI based data.

$$\text{ANI + PDS + ZP or MA} \underset{}{\overset{\Delta}{\rightleftharpoons}} \text{Composite}$$

$$\text{Composite} \underset{}{\overset{\Delta}{\rightleftharpoons}} \text{ANI + ZP or MA + } 2SO_4^{\circ-} \quad (R_1^{\circ})$$

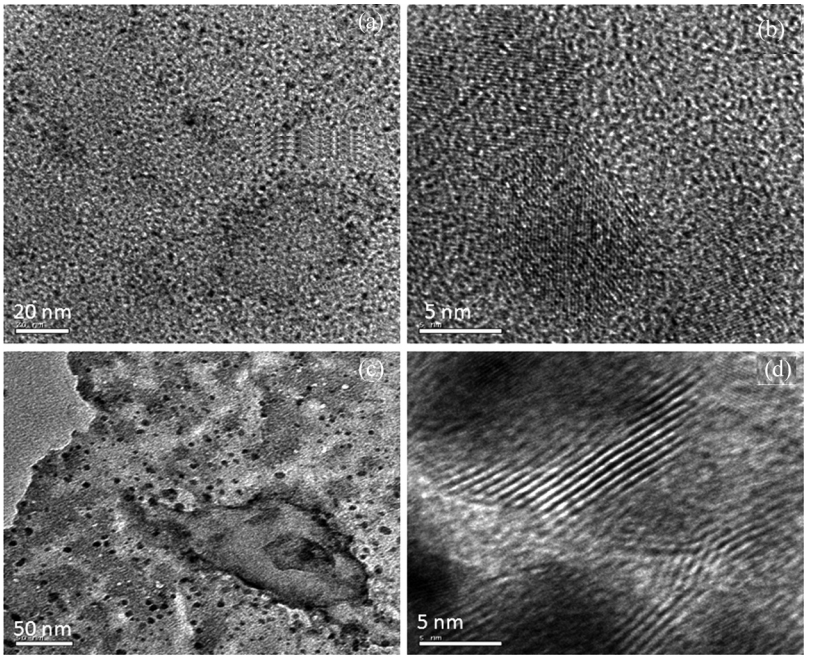

Figure 14: HRTEM of (a) ANI-PDS-ZP, (b) ANI-PDS-MA.

Initiation

$$\begin{aligned}
\mathrm{ANI} + \mathrm{SO_4^{o-}} &\longrightarrow \mathrm{ANI^{+o}} + \mathrm{HSO_4^-} \\
\mathrm{ANI} + \mathrm{MA_{ox}} &\longrightarrow \mathrm{ANI^{+o}} + \mathrm{Product} \quad \text{ox-oxidation} \\
\mathrm{ANI} + \mathrm{MA_{sce}} &\longrightarrow \mathrm{ANI^{+o}} + \mathrm{Product} \quad \text{sce-surface catalytic effect} \\
\mathrm{ANI} + \mathrm{ZP_{sce}} &\longrightarrow \mathrm{ANI^{+o}} + \mathrm{Product}
\end{aligned}$$

Propagation

$$\begin{aligned}
2\mathrm{ANI^{+o}} &\longrightarrow \mathrm{dimer} + \mathrm{H_2} \\
\mathrm{dimer} + \mathrm{R_1^o/MA/ZP} &\longrightarrow \mathrm{dimer^{+o}} + \mathrm{Product} \\
2\mathrm{dimer^{+o}} &\longrightarrow \mathrm{oligomer} \\
\mathrm{oligomer} + \mathrm{R_1^o/MA/ZP} &\longrightarrow \mathrm{oligomer^{+o}} + \mathrm{Product} \\
\mathrm{ANI} + \mathrm{MA/ZP} &\longrightarrow \mathrm{ANI\ intercalated\ MA/ZP} \\
\mathrm{oligomer} + \mathrm{ZP/MA} &\longrightarrow \mathrm{oligomer\ intercalated\ MA/ZP} \\
\mathrm{ANI} + \mathrm{ZP/MA_{host}} &\longrightarrow \mathrm{ANI\ intercalated\ MA/ZP}
\end{aligned}$$

Termination

$$2\,\text{oligomr}^{+o} \longrightarrow \text{Poly(ANI)} + H_2$$

During the preparation of polymer/nano composite, there is a chance for three types of reactions. They are intercalation, delamination and exfoliation reactions. Both the experimental results(first order dependence reactions) and HRTEM reports combinedly declared that during the polymer/nanocomposite formation, intercalation of polymer into the basal spacing of ZP or MA was formed. If the loading of nanosized ZP or MA was heavy, then agglomeration of nanoparticles occurred. Hence the follwoing mechanism is proposed here.

$$\begin{aligned}\text{Poly(ANI)} + \text{MA} &\longrightarrow \text{Poly(ANI)/MA nanocomposite}\\ &\longrightarrow \text{Poly(ANI)intercalated MA}\\ &\longrightarrow \text{Poly(ANI)exfoliated MA}\\ &\longrightarrow \text{Poly(ANI)delaminated MA}\end{aligned}$$

The similar type of mechanism was proposed for ANI-ZP system too.

$$2\text{oligomer}^{+o} + \text{MA/ZP}_{\text{dopant}} \longrightarrow \text{MA/ZP doped poly (ANI)}$$

The increased in electrical conductivity value back supported this reaction.

$$\begin{aligned}\text{Poly(ANI)}_{\text{aae}} + \text{MA/ZP} &\longrightarrow \text{MA/ZP dispersed on poly(ANI) matrix}\\ \text{Poly(ANI)} + \text{nMA/ZP} &\longrightarrow \text{agglomerated MA/ZP on poly(ANI) matrix}\end{aligned}$$

AAE-auto acceleration effect due to the active surface of formed poly(ANI). Auto acceleration effect of poly(ANI) was confirmed in our earlier publications [30–32]. The FTIR-RI measurements gave the following results.

$$\begin{aligned}\text{ANI} + 1\,\text{mol ZP} &\longrightarrow 1\,\text{mol benzenoid form}\\ \text{ANI} + 0.5\,\text{mol ZP} &\longrightarrow 1\,\text{mol quinonoid form}\\ \text{ANI} + 1\,\text{mol MA} &\longrightarrow 1\,\text{mol benzenoid form}\\ \text{ANI} + 1\,\text{mol MA} &\longrightarrow 1\,\text{mol quinonoid form}\end{aligned}$$

Based on the above kinetic reports, one can draw the structure of Poly(ANI) as mentioned below.

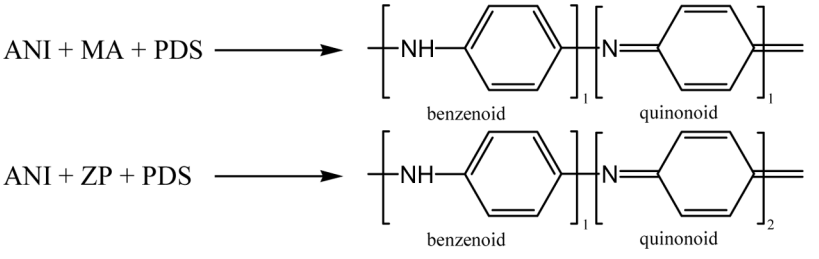

Due to the above mentioned structure, the ZP system must produce a higher electrical conductivity value, but unfortunately ZP acted as a poor dopant and resulted in lower electrical conductivity than the MA system.

CONCLUSIONS

From the above kinetic study, the important points are presented here in conclusion:

1. the free radical R_p of ANI was boosted in the presence of ZP rather than MA due to the surface catalytic effect;
2. the FTIR-RI values were also modified in the presence of nanosized ZP and MA;
3. the FTIR-RI values showed the 1.0 and 0.50 order dependence with respect to % weight of ZP for benzenoid and quinonoid structure of PANI;
4. while varied, the % weight of MA, the FTIR-RI exhibited the 1.0 order dependence for both benzenoid and quinonoid structure of PANI;
5. PANI exhibited higher electrical conductivity values than the POT system due to the absence of the steric effect;
6. the MA system represented higher thermal stability than the ZP system; and
7. HRTEM confirmed the size of ZP as 5–10 nm with uniform distribution on the PANI backbone.

REFERENCES

[1] Naikzad, L., Alibeigi, S., Vaezi, M. R., Yazdani, B., and Rahimpor, M. R. *Chem. Eng. Technol.* **32**, 861 (2009).

[2] Nesher, G., Aylien, M., Sandaki, G., Avnir, D., and Marom, G. *Adv. Funct. Mater.* **19**, 1293 (2009).

[3] Nighia, N. D., and Tung, N. T. *Synth. Met.* **159**, 831 (2009).

[4] Cheng, Q., Pavlinek, V., He, Y., Li, C., and Saha, P. *Colloid Polym. Sci.* **287**, 435 (2009).

[5] Sharma, B. K., Gupta, A. K., Khare, N., Dhavan, S. K., and Gupta, H. C. *Synth. Met.* **159**, 391 (2009).

[6] Yang, C., Li, H., Xiong, D., and Cao, Z. *React. Funct. Polym.* **69**, 137 (2009).

[7] Posudievsky, O. Y., Biskulova, S. A., and Pokhodenko, V. D. *J. Mater. Chem.* **12**, 1446 (2002).

[8] Sadek, A. Z., Wlodearski, W., Shin, K., and Kaner, R. B. *Synth. Met.* **158**, 29 (2008).

[9] Li, X., Wang, D., Cheng, G., Luo, Q., and Wang, Y. *Appl. Cat. B. Environ.* **81**, 267 (2008).

[10] Ma, J., Zhang, X., Yan, C., and Inou, H. *J. Mater. Sci.* **43**, 5534 (2008).

[11] Yilmaz, F., and Kucukyavuz, X. J. *Appl. Polym. Sc.* **111**, 680 (2009).

[12] Qi, Y. N., Xu, F., Sun, L. X., and Liu, Y. Y. *J. Therm. Anal. Calor.* **94**, 553 (2008).

[13] Anbarasan, R., Sivakumaravel, S., and Gopiganesh, C. *Intern. J. Polymeric Mater.* **55**, 803 (2006).

[14] Anbarasan, R., Anandhakrishnan, R., and Vivek, G. *Polym. Compos.* **29**, 949 (2008).

[15] Yelilarasi, A., Juliat Latha Jayakumari, J., Dhanalakshmi, V., and Anbarasan, R. *J. Chil. Chem. Soc.* (submitted).

[16] Hameed, S. F., and Allam, M. A. *J. Appl. Sci. Res.* **2**, 27 (2006).

[17] Chakraborty, S., Bandyopadhyay, S., Ameta, R., and Deuri, A. S. *Polym. Test.* **26**, 38 (2007).

[18] Svegl, F., and Orel, B. *Mat. Tech.* **37**, 29 (2003).

[19] Asimow, P. D., Stein, L. C., and Rinsman, G. R. *Am. Mineral.* **91**, 278 (2006).

[20] Parker, J. R., and Waddell, W. H. *J. Elast. Plast.* **28**, 140 (1996).

[21] Saule, M., Navarre, S., Babout, O., and Maillard, B. *Macromolecules* **36**, 7469 (2003).

[22] Saule, M., Navarre, S., Babout, O., and Maillard, B. *Macromolecules* **38**, 77 (2005).

[23] Navarre, S., and Maillard, B. *J. Polym. Sci. Part A. Chem. Ed.* **3**, 2957 (2000).

[24] Anbarasan, R., Babout, O., Dequiel, M., and Maillard, B. *J. Appl. Polym. Sci.* **97**, 761 (2005).

[25] Anbarasan, R., Babout, O., and Maillard, B. *J. Appl. Polym. Sci.* **97**, 766 (2005).

[26] Duraimurugan, K., Rathiga, S., Baskaran, I., and Anbarasan, R. *Chin. J. Polym. Sci.* **26**, 393 (2008).

[27] Radhika, S., Duraimurugan, K., Baskaran, I., Dhanalakshmi, V., and Anbarasan, R. *J. Mater. Sci.* **44**, 3542 (2009).

[28] Anbarasan, R., Anton Kumanan, S. A., Siva, R., and Dhanalakshmi, V. *Int. J. Pure Appl. Chem.* **4**, 47 (2009).

[29] Yelilarasi, A., Juliat Latha Jayakumari, J., Dhanalakshmi, V., and Anbarasan, R. *Polym. Polym. Compos.* **17**, 397 (2009).